PCCP

RSC Publishing

PAPER

View Article Online
View Journal | View Issue

Cite this: *Phys. Chem. Chem. Phys.*, 2013, **15**, 17993

Rotational motion of a single water molecule in a buckyball†

A. Barati Farimani, Yanbin Wu and N. R. Aluru*

Received 2nd August 2013,
Accepted 28th August 2013

DOI: 10.1039/c3cp53277a

www.rsc.org/pccp

Encapsulation of a single water molecule in a buckyball (C60) can provide fundamental insights into the properties of water. Investigation of a single water molecule is feasible through its solitary confinement in C60. In this paper, we performed a detailed study of the properties and dynamics of a single water molecule in a buckyball using DFT and MD simulations. We report on the enhancement of rotational diffusion and entropy of a water molecule in C60, compared to a bulk water molecule. H_2O@C60 has zero translational diffusion and terahertz revolution frequency. The harmonic, high amplitude rotation of a single water molecule in C60 is compared to stochastic behavior of bulk water molecules. The combination of large rotational and negligible translational motion of water in C60 creates new opportunities in nanotechnology applications.

Introduction

Encapsulation of a single water molecule inside a buckyball opens up new opportunities to probe the properties of a single water molecule in great detail.[1] Most of the anomalous properties of bulk water such as the high boiling and melting points are associated with its hydrogen bond network.[2] Unlike bulk water, a single water molecule in a confined environment does not interact with other water molecules.[3,4] Trapping a single water molecule in a confined environment provides a unique opportunity to understand the physics of the single water molecule and its intrinsic novel properties. The diffusion barrier of a water molecule from outside of C60 to inside is too large, and techniques such as heating up of the C60 and water molecules would not help encapsulate the water molecule. Isolating a single water molecule inside C60 is possible through a molecular surgical approach.[5,6] The water accessible space inside a C60 can accommodate a single water molecule considering the maximum distance of water hydrogens, H···H = 1.67 Å. The buckyball is the smallest fullerene molecule containing pentagonal and hexagonal rings in which no two pentagons share an edge.[7] The C60 form of the carbon chain has the most natural occurrence and can be found in soot. C60 is soluble in many nonpolar solvents, like carbon sulfide and benzene, and it normally produces violet-colored solution. C60 is not soluble in water and several efforts have focused on modifications to the surface of the fullerene to enhance its solubility in water for biological and drug delivery applications.[8] Inserting water in C60 can pave the way for modifying the highly symmetrical, non-polar C60. So far, a few non-polar molecules, such as the nitrogen atom[9] and the hydrogen molecule,[10] were placed inside C60 to study their dynamics and electronic structure. But formation of H_2O@C60 (combination of non-polar C60 and polar water) may have several applications such as new electronic devices, molecular memories, single molecule transistors, high frequency resonators,[11] *etc.* The carbon atoms of endohedral fullerene can be modified, *e.g.* by attaching functional groups, to control and manipulate the water molecule movement.[12] Dynamics of single water and its signatures occur over a femtosecond timescale and existing experimental devices may not be able to fully capture its motion while the molecule is shielded *via* the cage.[13] Density functional theory (DFT) and molecular dynamics (MD) simulation can shed light on the dynamics and properties of a single water molecule inside the cage. The DFT method can predict interaction energy between C60 and the water molecule, dipole moment, and O–H bond vibrational frequencies. Some studies were performed on the dipole moment of H_2O@C60, which show that the dipole moment is not affected by encapsulation.[1,14] In contrast, Ensing *et al.*[15] observed that the dipole moment of H_2O@C60 decreased by a factor of 4. MD can predict the dynamics of water inside C60, thermodynamic properties and O–H bond vibrational frequencies, specifically at room temperature. MD simulation of a single water molecule inside C60 needs special care in comparison with bulk water simulation. The water model and C–water force field calibration for bulk systems may not be suitable to

Department of Mechanical Science and Engineering, Beckman Institute for Advanced Science and Technology, University of Illinois at Urbana-Champaign, Urbana, Illinois 61801, USA. E-mail: aluru@illinois.edu; Web: https://www.illinois.edu/~aluru/

† Electronic supplementary information (ESI) available. See DOI: 10.1039/c3cp53277a

describe the H_2O@C60 system. Studies need to be performed to obtain the appropriate water model and C–water force field using *ab initio* methods. The C–water interactions are all based on a pair-additive Lennard-Jones (LJ) potential between the atoms of water and the carbon atoms. The functional form of the potential is $V_{ij}^{6-12} = 4\varepsilon[(\sigma/R_{ij})^{12}-(\sigma/R_{ij})^{6}]$, where R_{ij} is the separation distance between a pair of atoms of water and carbon atoms, ε is the depth of the potential well, and $2^{1/6}\sigma$ is the position of the potential well. In this paper, DFT is used to design water force fields, which are then used in MD. Using DFT, the O–H bond vibrational frequencies, dipole moments and potential of a single water molecule in confinement are computed. The dynamic properties of a single water molecule such as diffusion coefficient, rotational diffusion coefficient, entropy, bond length and O–H bond vibrational frequencies are studied using MD.

Methods

In our simulations, we used both MD and DFT in conjunction to model the single water molecule in C60. In our recent work,[16] we developed C–water interaction parameters based on the DFT-SAPT *ab initio* data.[17] Here, we show that the C–water interaction parameters developed in ref. 16 can predict the water O–H stretching frequency shift reasonably well.

The interaction energies between C60 and a single water molecule, dipole moments, and water O–H bond vibrational frequencies are computed using DFT. DFT calculations were performed with the M06-2X functional and the 6-311G(2d,p) basis set. The M06-2X functional has been validated by Pascal *et al.*[18] for graphite by considering experimental data for mechanical and thermodynamic properties. M06-2X/6-311G(2d,p) gives benzene–water binding energy of 3.597 kcal mol^{-1}, compared to 3.247 kcal mol^{-1} by CCSD(T)/CBS. The difference is around 0.35 kcal mol^{-1}, which agrees with the mean error of 0.32 kcal mol^{-1} when the M06-2X functional was tested for the S22 non-covalent database[19] of biological importance.[20] The counterpoise method[21] was used to eliminate the basis set superposition errors. The dipole moments of H_2O@C60, C60 and water were obtained using the CHelpG scheme[22] by fitting atomic point charges to the electrostatic potential computed by DFT with the M06-2X functional. The dipole moments of H_2O@C60, C60, and water are 0.468, 0.0, and 2.06 Debye, respectively. The dipole moment of H_2O@C60 is about one quarter of that of bulk water, which is consistent with the results of Ensing *et al.*[15] This screening effect of C60 on water was also observed for other gas molecules[23] like H_2, N_2, and CO. The O–H bond vibrational frequencies are obtained using normal mode analysis based on the potential energy surface from DFT calculations. The calculated O–H bond vibrational frequencies are corrected by a scaling factor of 0.9441 to account for the anharmonicity of the potential. The anharmonicity corrections are important for the calculation of vibrational frequencies. Without the anharmonicity corrections, the root mean square (RMS) difference between computed frequencies by DFT and experimental frequencies for F38/10 database is 148 cm^{-1}. With the anharmonicity corrections, the RMS difference is 47 cm^{-1} (see section "Scaling factor for M06-2X/6-311G(2d,p) frequencies", ESI†). All DFT and CCSD(T) calculations are done using Gaussian.[24]

A flexible water model is needed in MD to capture the O–H stretching, H–O–H bending and correct dynamics of a single water molecule. The accuracy of various flexible water models, such as flexible SPC/E,[25,26] SPC, TIP3P,[26,27] and Ferguson[28] water models, is tested with experimental gas-phase O–H bond vibrational frequencies of water.[29]

Compared to a water molecule in gas phase, a single water molecule inside C60 has different O–H bond vibrational behavior because of its interactions with carbon atoms in C60. This difference can be quantified by the O–H bond vibrational frequency shift from the gas-phase water. MD simulations can be used to compute the O–H bond vibrational frequency shift. A comparison between the DFT and MD results can be used to evaluate the accuracy of C–water MD interaction parameters in confinement. In MD, the water O–H bond vibrational frequencies inside C60 are obtained from the water power spectra. Each vibrational mode frequency corresponds to a peak position in the water power spectra, which is a Fourier transformation of the velocity autocorrelation of hydrogen atoms (see section "Frequency calculation in MD", ESI†). The velocity autocorrelation was averaged over 200 runs with different water initial geometry and velocity to reduce the error bar of frequencies to around 2 wave numbers.

Molecular dynamics simulations were performed using LAMMPS.[30] A schematic of the simulation setup is shown in Fig. 1a. Temperature was maintained at 300 K by applying the Nosé–Hoover[31,32] thermostat with a time constant of 0.01 ps. The cutoff distance for the LJ interactions is 15 Å. The long-range electrostatic interactions were computed by using the particle mesh Ewald method (real space cutoff, 10 Å; reciprocal space gridding, 1.2 Å, fourth-order interpolation). The C60 structure was relaxed using DFT with PBE functional and double-zeta polarized basis set and icosahedral geometry of C60 was maintained. We took the relaxed geometry of C60 from DFT and used it in MD simulations. Carbon atoms were frozen to their lattice position to prevent out-of-plane displacement.[33] We tested the non-frozen carbon atoms and the results did not change. Time integration was performed by applying the Verlet algorithm with a time step of 0.1 fs (tests were also performed with 0.01 fs and there is no change in results). The energy minimization is performed and simulations were run for 200 ns (see video V.1, ESI†). The data were collected every 1 fs to track the motion and O–H bond vibrational frequencies of a single water molecule. Our observations show that collecting the data with bigger time steps wouldn't be able to capture the rotational dynamics of water. It is notable that with *ab initio* MD, it is only possible to run less than 100 ps with current computational power. Our observation shows that at initial stages of simulation ($t < 500$ ps), thermal noise is high and the temperature fluctuations of the water molecule are large.[14]

Results and discussion

First, we used SPC/E, SPC, TIP3P and Ferguson flexible water models to compute the gas-phase O–H bond vibrational

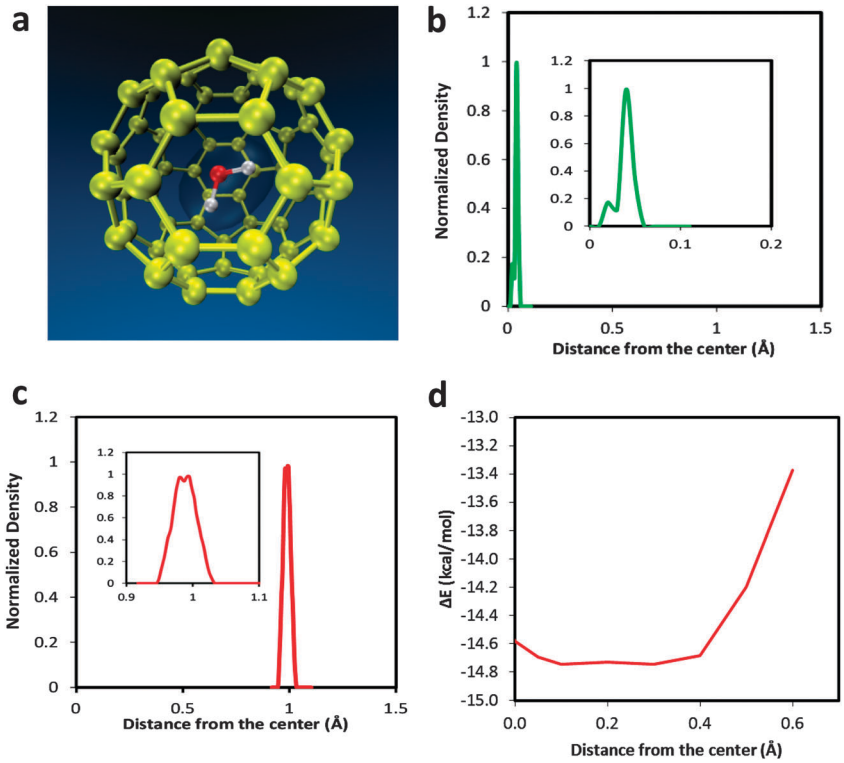

Fig. 1 (a) Simulation of a single water molecule inside C60. This configuration is used both in MD and DFT simulations. (b) Radial distribution of oxygen obtained from MD simulations (200 ns runtime) inside C60, the inset shows the exact location of oxygen and the offset of 0.05 Å from the center is observed. (c) Radial distribution of hydrogen atoms obtained from MD simulations inside C60, in inset, two peaks represent the stretching modes of hydrogen atoms. (d) DFT calculation of potential energy with respect to the position of oxygen atom in C60.

frequencies and compared them with experimental data (see section "Gas-phase O–H bond vibrational frequencies of water", ESI†). We find that the flexible Ferguson water model gives the best match with experiments.[28] Two C–water interaction parameters are used in MD to compute the frequency shift of the water stretching modes: first, the parameters obtained by fitting to the DFT–SAPT graphene–water interaction curve[16,17] (denoted as "MD1") and second, by applying the Lorentz–Berthelot combinational rule to carbon parameters from AMBER[34] and oxygen parameters from TIP3P water model[35] (denoted as "MD2"). The parameters for MD1 and MD2 are tabulated in Table 1. The carbon–hydrogen vdW interaction is non-zero for MD1 parameters and so the water–C60 interaction has C_{2v} symmetry. The MD2 C–water parameters were used by Hummer *et al.*[36] to study water conduction through a carbon nanotube. The frequency shift predicted by DFT calculations with M06-2X functional, MD1, and MD2 are summarized in Table 2.

The MD2 C–water parameters give zero frequency shift. It can be shown that if the carbon and water hydrogen ε_{C-HW} is zero, then the frequency shift is always zero. This zero frequency shift doesn't depend on the carbon and water oxygen interaction parameter, ε_{C-OW}. As indicated by DFT calculations,[1,37] the C60–water interaction induces non-zero frequency shift on water stretching modes. The MD1 C–water parameters predict a blue shift of 15 cm^{-1} in the asymmetric stretching mode and 14 cm^{-1} in the symmetric stretching mode, as shown in Fig. 2 and Table 2. Our calculation shows that the difference between vibrational kinetic energies ($E_{vib} = E_{tot} - E_{trans} - E_{rot}$, where E_{tot}, E_{trans}, and E_{rot} are total, translation, and rotational kinetic energies of water, respectively) in gas phase and in C60 is, $E_{vib,gasph} - E_{vib,H_2O@C60} = 0.9$ kJ mol^{-1} which corresponds to the blue shift.

Table 2 Frequency shifts using DFT with M06-2X functional, MD1, and MD2. The force field parameters for MD1 and MD2 are described in Table 1

Vibrational mode	DFT	MD1	MD2
Asymmetrical stretching shift (cm^{-1})	−84	15	0
Symmetrical stretching shift (cm^{-1})	−72	14	0

Table 1 C–water interaction parameters used in this work. The water intra-molecular interaction is described by the Ferguson water model[28] for both MD1 and MD2. The unit for σ_{C-OW} and σ_{C-HW} is Å, and the unit for ε_{C-OW} and ε_{C-HW} is kcal mol^{-1}

Ref.	C–water model	σ_{C-OW}	ε_{C-OW}	σ_{C-HW}	ε_{C-HW}
MD1[16]	Fitting to DFT-SAPT *ab initio* graphene–water interaction curve	3.372	0.1039	2.640	0.0256
MD2[36]	Combinational rule to carbon parameters from AMBER and oxygen parameters from TIP3P water model	3.275	0.1143	N/A	N/A

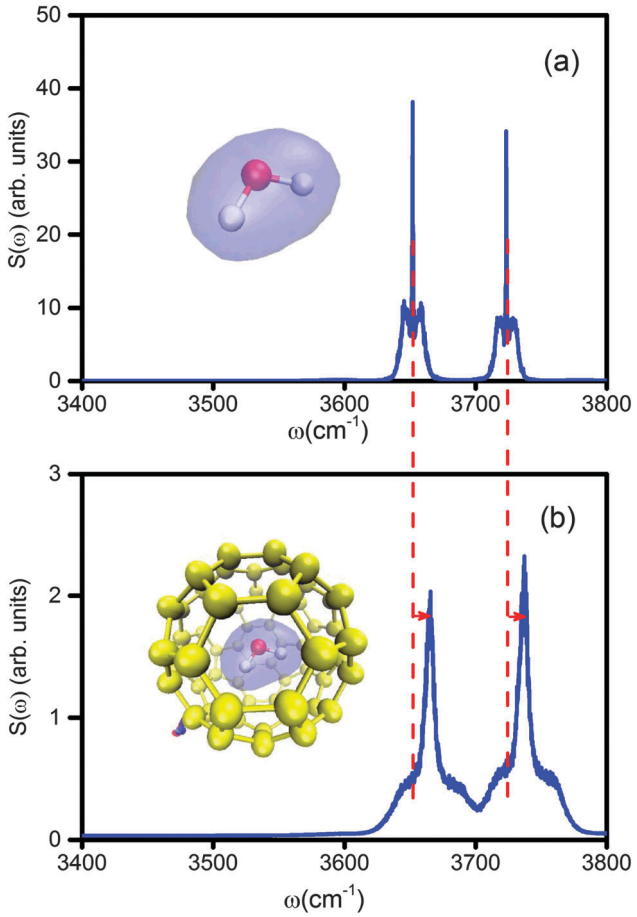

Fig. 2 Power spectra obtained from MD for (a) a single water molecule in the gas phase (b) a single water molecule inside C60. The two peaks in each figure correspond to symmetric stretching mode (left) and asymmetric stretching mode (right). The difference between the dashed lines and peaks in Fig. 2b shows the frequency shift. 200 simulations with different water initial geometry and velocity were performed to reduce the error bar to 2 wave numbers.

Non-zero C–water hydrogen ε_{C-HW} is essential to capture the appropriate vibrational motion of the hydrogen atoms. Bucher[14] used a rigid water model in his MD calculation which could not predict the vibrational frequency shift. As this study focuses on the rotational motion of the water molecule inside C60, a proper description of the dynamics of hydrogen atoms is important. Hence, in this work, we will use the MD1 C–water interaction parameters.

To locate the exact position of water inside C60, we spherically binned the cage (400 bins) and registered the position of oxygen and the two hydrogens. The density of oxygen and hydrogens (normalized by their maximum density) are shown in Fig. 1b and c, respectively. The oxygen atom is not located exactly at the center of C60. There is a shift of around 0.05 Å between the center of the buckyball and the oxygen atom. Hydrogen atoms are located at 1 Å distance from the center. In the inset of Fig. 1c, for the hydrogen density, two peaks are observed. These peaks represent the stretching of the hydrogen atoms. The distance between the two peaks is 0.2 Å. We averaged the (O···H) bond length of water for 5 simulation runs (each 200 ns) in C60 and observed a very small stretching difference of this bond (0.096 Å) compared to bulk (see Table 3). The small increase in bond length shows that the attraction of hydrogen toward the cage causes the slight stretch. The center of mass of the water molecule is not located at the center of C60. The interaction energy between C60 and a single water molecule as a function of the distance of oxygen from the center of C60 is calculated by DFT with M06-2X functional. The water molecule is orientated such that the dipole moment of the water molecule is always pointing towards the center of C60. The potential is not symmetric about the center of the C60. The potential is shown in Fig. 1d. A small potential barrier of 0.1 kcal mol^{-1} is observed at the center of C60 which justifies the 0.05 Å shift of oxygen's position from the center of C60.

Our calculation shows that the translational diffusion coefficient of water is $D_{trans,H_2O@C60} = 4.544 \times 10^{-15}$ cm^2 s^{-1}, which is negligible in comparison to the diffusion coefficient of bulk water, $D_{trans,bulk} = 2.441 \times 10^{-5}$ cm^2 s^{-1}. The mechanism of diffusion for bulk water is Fickian, and in carbon nanotubes with diameters smaller than 1 nm is single file (medium confinement).[38] In C60, the mechanism for water translation is stationary vibration. The translational entropy of water in a buckyball using the quasi harmonic oscillation method[39] is $S_{trans,H_2O@C60} = 8.48 \times 10^{-6}$ J mol^{-1} K which is negligible in comparison to the bulk value of $S_{trans,bulk} = 58.08$ J mol^{-1} K. The translational entropy of bulk water using the 2PT model[40] is $S_{trans,bulk} = 49.87$ J mol^{-1} K. The translational entropy and diffusion indicate that confinement restricts the translational motion of a water molecule.

The average number of hydrogen bonds per water molecule in bulk is 3.41, in contrast to zero O–H···O hydrogen bonds for a single water molecule in C60.[41] The O–H···O hydrogen bonds

Table 3 Comparison of properties obtained using MD: H_2O@C60 and bulk H_2O (water model: flexible Ferguson model). $\langle|\omega|\rangle$ is the averaged absolute angular frequency of water molecules

Properties	Water in C60	Bulk water
Translational diffusion ($\times 10^{-5}$ cm^2 s^{-1})	4.544×10^{-10}	2.441
Rotational diffusion (rad^2 ps^{-1})	32.56	3.46
Hydrogen bond (n)	0	3.41
O···H (Å)	1.0002	0.94634
HOH (°)	109.64	108.87
Translational entropy (J mol^{-1} K)	8.48×10^{-9}	49.87–57.0822
$\langle|\omega_x|\rangle$, $\langle|\omega_y|\rangle$, $\langle|\omega_z|\rangle$ (THz)	1.44, 1.22, 1.45	0.17, 0.13, 0.17
Rotational entropy	$8.78K_B$	$1.38K_B$

and the water–water interactions limit the rotational movement of water molecules in bulk. The nature of intermolecular interactions (both LJ and electrostatic) in bulk water doesn't constrain the translational motion but it limits the rotational motion. In contrast, the water molecule's translational motion is significantly damped in C60, while its rotational motion is not hindered (see video V.1, ESI†). We computed the rotational diffusion coefficient of a single water molecule in C60 and it is found to be $D_{rot,H_2O@C60} = 33.56$ rad^2 ps^{-1}. The rotational diffusion coefficient of a water molecule in bulk[42] is 3.46 rad^2 ps^{-1} (see section ''Rotational diffusion'', ESI†). A single water molecule's rotational diffusion coefficient is 9–10 times larger than its bulk value. In Fig. 3a, the dipole angle with respect to an arbitrary axis is shown *versus* time. The dipole distribution shows that the water molecule rotates freely. The interaction energies between C60 and the water molecule with respect to orientation of the water molecule are computed by DFT and shown in Fig. 3b. The energy barrier for the rotational motion of water is less than 0.2 kcal mol^{-1}, which is about a third of k_BT at 300 K. This explains the free rotation of water inside C60 observed in MD.[43] Jose and Datta[44] showed that a methanol–ethanol molecule inside cavitands has rapid rotational motion due to a small energy barrier within the cavitands, which is similar to our observation of fast rotation of a single water molecule inside C60. In Fig. 3c, the dipole rotational autocorrelation functions (RACF) for bulk water and H_2O@C60 are shown. RACF indicates that water molecules in bulk tend to keep their orientations up to 10 ps while in C60, reorientation occurs in femtosecond timescale. HB network hinders the rotation of water in bulk. For water clusters in small diameter carbon nanotubes ((8, 8) CNT, (9, 9) CNT, ice-like CNTs), the RACF relaxation time is of the order 40–50 ps. In these clusters, long lifetime hydrogen bonds lock the rotational motion of molecules as it also occurs in the crystal ice.[45] The hydrogen atoms are at a distance of 2.643 Å from the cage carbon atoms showing that there could be weak O–H$\cdots\pi$ interaction between the hydrogen atoms and the π electron cloud of the cage. This has been shown by Ramachandran and Sathyamurthy[46] using

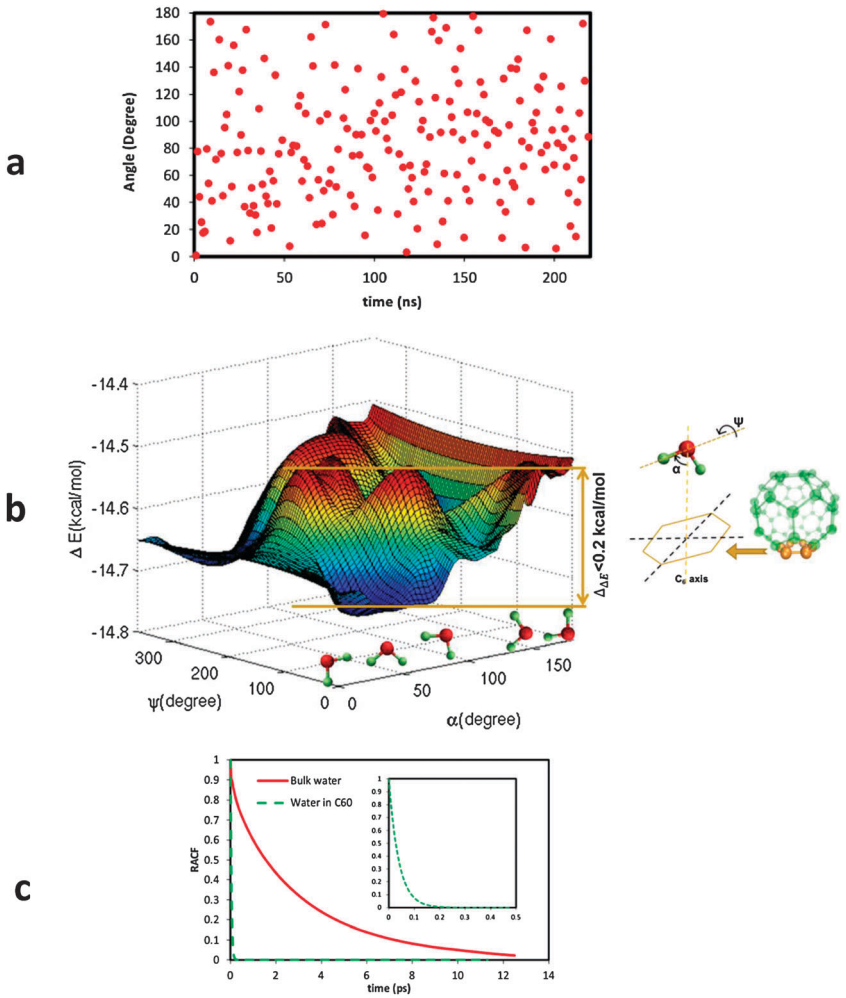

Fig. 3 (a) Dipole angle distribution with respect to time obtained from MD simulations. (b) The DFT interaction energy between C60 and a single water molecule for various water orientations. α represents the rotation of the water molecule within the water plane (the orange dashed line is the C_6 axis of one arbitrarily chosen hexagonal ring of C60) and ψ represents the rotation of the water molecule along one O–H bond (see details in ESI†). (c) Rotational autocorrelation of the dipole for water molecules in C60 and in bulk obtained from MD, inset is the zooming in 0–1 ps time.

the atoms-in-molecules method. Ramachandran's calculation shows that the water molecule is slightly constrained inside the fullerene cage due to the O–H···π interaction. Our frequency shift calculation also confirms that water O–H bond frequency and length is affected by the O–H···π interaction. O–H···π (pentagonal ring) is similar to O–H···π (hexagonal ring) since water molecule doesn't show any specific preference in orienting toward each of them from our DFT calculations (see Fig. 3). Our DFT calculations of interaction energies between C60 and water for various water orientations show a small energy difference of 0.2 kcal mol^{-1}, which is the upper limit of the energy difference among all the possible orientations of water in C60. Therefore the energy difference between O–H···π (pentagonal ring) and O–H···π (hexagonal ring) is no more than 0.2 kcal mol^{-1}. The O–H···π is not as stable as O–H···O. This can be understood from the rotational diffusion coefficient comparison of H_2O@C60 and water in bulk (see Table 3). The rotational diffusion coefficient of H_2O@C60 is ten times larger than that of water in bulk, which shows that the O–H···π is not as stable as O–H···O. In Table 3, the ∢HOH angle of water is reported in bulk and in C60. The ∢HOH angle is slightly increased (0.8°) because of C···H interaction. With zero C–H interaction, no change in the mean value of ∢HOH angle is observed.

Experiments have also shown that water rotates continuously inside a C60[1]. We have estimated the rotational entropy of water molecules in bulk and compared it with H_2O@C60 (see section "Rotational entropy", ESI†). The results show that the rotational entropy of a single water molecule in C60 is 6.5 times greater than that of bulk (see Table 3). Rotation of water in C60 has huge entropic gain. Our calculations also show that 83% of the total kinetic energy is spent on the rotation of water, less than 1% is spent on translation and the rest goes to vibrational kinetic energy of water in C60. In bulk, the rotational contribution of kinetic energy is less than 5%. The average absolute angular velocities of water inside C60 show terahertz frequencies (Table 3), in contrast with bulk water, where molecules can hardly make

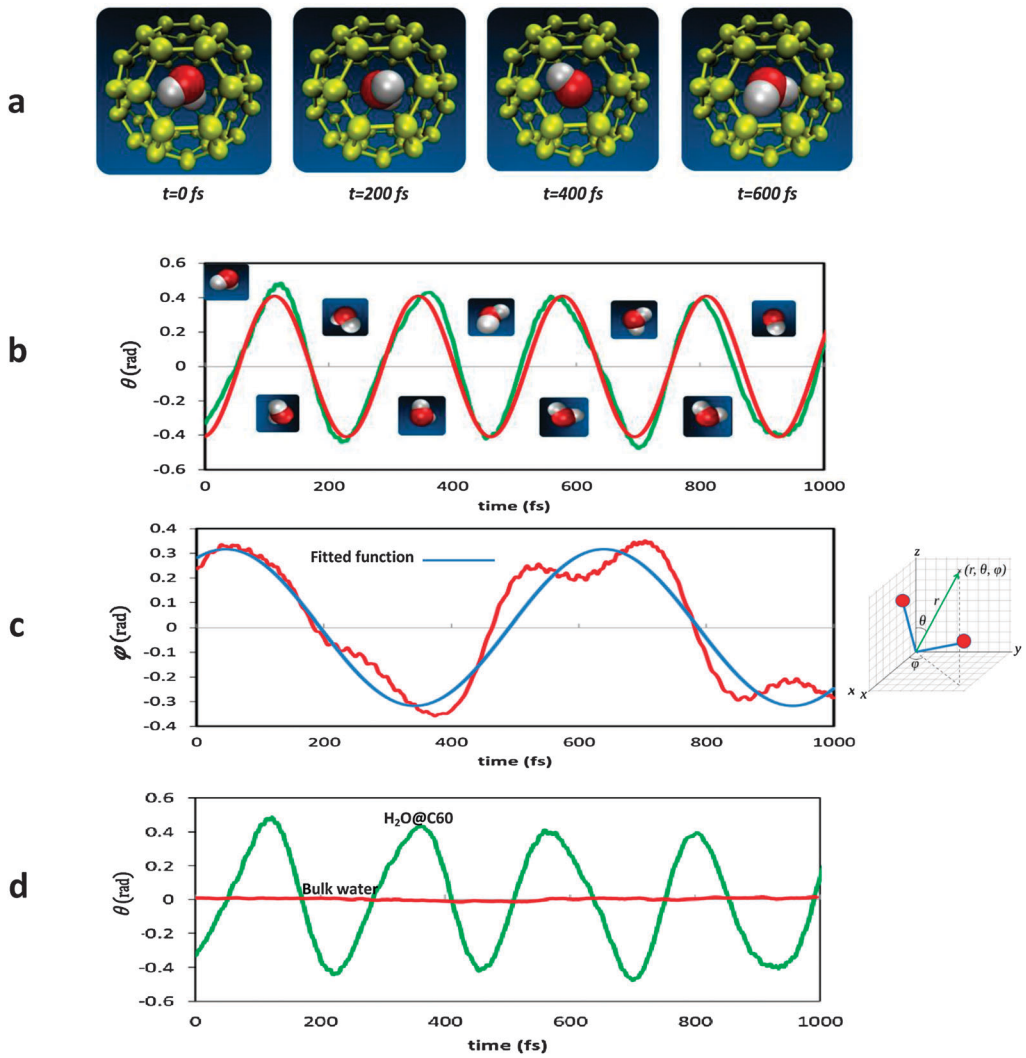

Fig. 4 (a) Snapshots of orientation of a water molecule inside buckyball at different times. These results are taken from MD simulations with a time step of 0.1 fs. (b) Characteristic motion of H_2O@C60 in the θ direction. (c) Characteristics motion characteristic of H_2O@C60 in the φ direction and the representation of θ and ϕ directions of the water dipole. (d) Comparison of bulk water molecules' motion *versus* H_2O@C60.

a full revolution. The large rotational frequencies of water in C60 can be exploited for applications such as resonators and single molecule switches.

To understand the dynamics of water motion, the dipole vector of water in C60 is mapped into spherical coordinates and the motion is projected in φ and θ planes (see Fig. 4c). The type of motion is sinusoidal with the highest amplitude of 0.41 rad and 0.31 rad in φ and θ directions, respectively. The best functions to describe the motion of water in C60, in θ and φ planes are $\theta = 0.41 \sin(0.027t - 1.462)$ and $\varphi = 0.3116 \sin(0.0106t + 1.086)$, respectively. The same procedure is repeated for a single molecule in bulk water and the average values of motion (amplitude and frequency) were extracted. In bulk, the highest amplitudes are 0.02 and 0.01 rad in φ and θ directions, respectively. Fig. 4 shows the motion in these two planes. Fig. 4a and b show the motion in θ and φ directions for H_2O@C60. In Fig. 4c the amplitude and the motion of water molecules in bulk are compared to H_2O@C60. The amplitude of the rotational motion of water in bulk is very small (<0.1 rad) compared to a single water molecule in C60. The rotational dynamics of water molecules in bulk doesn't follow any pattern (see Fig. 4d inset). In summary, the rotational motion of water in bulk is stochastic while the rotational motion of water in C60 is harmonic.

Conclusions

To understand the dynamics of a single water molecule and its properties in C60, we have designed and tested the water–carbon model and force field in MD. Dynamics and properties of H_2O@C60 (dipole moment, density, *etc.*) were extracted and compared to bulk. In comparison to bulk, the rotational diffusion coefficient is enhanced by about an order of magnitude and the rotational entropy is enhanced by 6.5 times. Non-hydrogen bonded water's translational diffusion is near zero which makes it suitable to read its dipole angular status. A single water molecule in C60 exhibits a harmonic and a high amplitude motion with a terahertz revolution frequency. The stagnant single molecule with huge rotational motion can find wide spread applications in various disciplines.

Acknowledgements

This work is supported by AFOSR and NSF under grants 0852657, 0915718 and 1264282. The authors gratefully acknowledge the use of the parallel computing resource provided by the University of Illinois. This work used the Extreme Science and Engineering Discovery Environment (XSEDE), which is supported by the National Science Foundation Grant Number OCI-1053575.

References

1 K. Kurotobi and Y. Murata, *Science*, 2011, **333**(6042), 613–616.
2 R. Ludwig, *Angew. Chem., Int. Ed.*, 2001, **40**(10), 1808–1827.
3 J. Garric, J.-M. Leger and I. Huc, *Chem.–Eur. J.*, 2007, **13**(30), 8454–8462.
4 T. H. Noh, E. Heo, K. H. Park and O.-S. Jung, *J. Am. Chem. Soc.*, 2011, **133**(5), 1236–1239.
5 Y. Rubin, *Chem.–Eur. J.*, 1997, **3**(7), 1009–1016.
6 N. J. Turro, J. Y. C. Chen, E. Sartori, M. Ruzzi, A. Marti, R. Lawler, S. Jockusch, J. López-Gejo, K. Komatsu and Y. Murata, *Acc. Chem. Res.*, 2009, **43**(2), 335–345.
7 H. W. Kroto, J. R. Heath, S. C. Obrien, R. F. Curl and R. E. Smalley, *Nature*, 1985, **318**(6042), 162–163.
8 A. L. Balch, *Science*, 2011, **333**(6042), 531–532.
9 B. Pietzak, M. Waiblinger, T. A. Murphy, A. Weidinger, M. Hohne, E. Dietel and A. Hirsch, *Chem. Phys. Lett.*, 1997, **279**(5–6), 259–263.
10 K. Komatsu, M. Murata and Y. Murata, *Science*, 2005, **307**(5707), 238–240.
11 W. Harneit, *Phys. Rev. A*, 2002, **65**(3), 032322, DOI: 10.1103/PhysRevA.65.032322.
12 S. Vijayaraghavan, D. Ecija, W. Auwaerter, S. Joshi, K. Seufert, A. P. Seitsonen, K. Tashiro and J. V. Barth, *Nano lett.*, 2012, **12**(8), 4077–4083.
13 C. Beduz, M. Carravetta, J. Y. C. Chen, M. Concistre, M. Denning, M. Frunzi, A. J. Horsewill, O. G. Johannessen, R. Lawler, X. G. Lei, M. H. Levitt, Y. J. Li, S. Mamone, Y. Murata, U. Nagel, T. Nishida, J. Ollivier, S. Rols, T. Room, R. Sarkar, N. J. Turro and Y. F. Yang, *Proc. Natl. Acad. Sci. U. S. A.*, 2012, **109**(32), 12894–12898.
14 D. Bucher, *Chem. Phys. Lett.*, 2012, **534**, 38–42.
15 B. Ensing, F. Costanzo and P. L. Silvestrelli, *J. Phys. Chem. A*, 2012, **116**(49), 12184–12188.
16 Y. Wu and N. R. Aluru, *J. Phys. Chem. B*, 2013, **117**(29), 8802–8813.
17 G. R. Jenness, O. Karalti and K. D. Jordan, *Phys. Chem. Chem. Phys.*, 2010, **12**(24), 6375–6381.
18 T. A. Pascal, N. Karasawa and W. A. Goddard, 3rd, *J. Chem. Phys.*, 2010, **133**(13), 134114.
19 P. Jurecka, J. Sponer, J. Cerny and P. Hobza, *Phys. Chem. Chem. Phys.*, 2006, **8**(17), 1985–1993.
20 Y. Zhao and D. G. Truhlar, *Theor. Chem. Acc.*, 2008, **120**(1–3), 215–241.
21 S. F. Boys and F. Bernardi, *Mol. Phys.*, 1970, **19**(4), 553–566.
22 C. M. Breneman and K. B. Wiberg, *J. Comput. Chem.*, 1990, **11**(3), 361–373.
23 J. Cioslowski, *J. Am. Chem. Soc.*, 1991, **113**(11), 4139–4141.
24 M. J. Frisch, G. W. Trucks, H. B. Schlegel, G. E. Scuseria, M. A. Robb, J. R. Cheeseman, J. A. Montgomery Jr, T. Vreven, K. N. Kudin, J. C. Burant, J. M. Millam, S. S. Iyengar, J. Tomasi, V. Barone, B. Mennucci, M. Cossi, G. Scalmani, N. Rega, G. A. Petersson, H. Nakatsuji, M. Hada, M. Ehara, K. Toyota, R. Fukuda, J. Hasegawa, M. Ishida, T. Nakajima, Y. Honda, O. Kitao, H. Nakai, M. Klene, X. Li, J. E. Knox, H. P. Hratchian, J. B. Cross, V. Bakken, C. Adamo, J. Jaramillo, R. Gomperts, R. E. Stratmann, O. Yazyev, A. J. Austin, R. Cammi, C. Pomelli, J. W. Ochterski, P. Y. Ayala, K. Morokuma, G. A. Voth, P. Salvador, J. J. Dannenberg, V. G. Zakrzewski, S. Dapprich, A. D. Daniels, M. C. Strain, O. Farkas, D. K. Malick, A. D. Rabuck, K. Raghavachari, J. B. Foresman, J. V. Ortiz, Q. Cui, A. G. Baboul, S. Clifford,

J. Cioslowski, B. B. Stefanov, G. Liu, A. Liashenko, P. Piskorz, I. Komaromi, R. L. Martin, D. J. Fox, T. Keith, M. A. Al-Laham, C. Y. Peng, A. Nanayakkara, M. Challacombe, P. M. W. Gill, B. Johnson, W. Chen, M. W. Wong, C. Gonzalez and J. A. Pople, Gaussian, Inc., Wallingford, CT, 2004.

25 H. J. C. Berendsen, J. R. Grigera and T. P. Straatsma, *J. Phys. Chem.*, 1987, **91**(24), 6269–6271.

26 E. Lindahl, B. Hess and D. van der Spoel, *J. Mol. Model*, 2001, **7**(8), 306–317.

27 P. Mark and L. Nilsson, *J. Phys. Chem. A*, 2001, **105**(43), 9954–9960.

28 D. M. Ferguson, *J. Comput. Chem.*, 1995, **16**(4), 501–511.

29 S. H. Chen, K. Toukan, C. K. Loong, D. L. Price and J. Teixeira, *Phys. Rev. Lett.*, 1984, **53**(14), 1360–1363.

30 S. Plimpton, *J. Comput. Phys.*, 1995, **117**(1), 1–19.

31 S. Nosé, *J. Chem. Phys.*, 1984, **81**(1), 511–519.

32 W. G. Hoover, *Phys. Rev. A*, 1985, **31**(3), 1695–1697.

33 I. Hanasaki and A. Nakatani, *J. Chem. Phys.*, 2006, **124**(14), 144708, DOI: 10.1063/1.2187971.

34 W. D. Cornell, P. Cieplak, C. I. Bayly, I. R. Gould, K. M. Merz, D. M. Ferguson, D. C. Spellmeyer, T. Fox, J. W. Caldwell and P. A. Kollman, *J. Am. Chem. Soc.*, 1995, **117**(19), 5179–5197.

35 W. L. Jorgensen, J. Chandrasekhar, J. D. Madura, R. W. Impey and M. L. Klein, *J. Chem. Phys.*, 1983, **79**(2), 926–935.

36 G. Hummer, J. C. Rasaiah and J. P. Noworyta, *Nature*, 2001, **414**(6860), 188–190.

37 O. Shameema, C. N. Ramachandran and N. Sathyamurthy, *J. Phys. Chem. A*, 2006, **110**(1), 2–4.

38 A. B. Farimani and N. R. Aluru, *J. Phys. Chem. B*, 2011, **115**(42), 12145–12149.

39 A. A. Polyansky, R. Zubac and B. Zagrovic, Estimation of Conformational Entropy in Protein–Ligand Interactions: A Computational Perspective, in *Computational Drug Discovery and Design*, ed. R. Baron, 2012, vol. 819, pp. 327–353.

40 S.-T. Lin, P. K. Maiti and W. A. Goddard, III, *J. Phys. Chem. B*, 2010, **114**(24), 8191–8198.

41 Y. Wu, S. Joseph and N. R. Aluru, *J. Phys. Chem. B*, 2009, **113**(11), 3512–3520.

42 A. Debnath, B. Mukherjee, K. G. Ayappa, P. K. Maiti and S.-T. Lin, *J. Chem. Phys.*, 2010, **133**(17), 174704, DOI: 10.1063/1.3494115.

43 A. Varadwaj and P. R. Varadwaj, *Chem.–Eur. J.*, 2012, **18**(48), 15345–15360.

44 D. Jose and A. Datta, *J. Phys. Chem. Lett.*, 2010, **1**(9), 1363–1366.

45 R. J. Mashl, S. Joseph, N. R. Aluru and E. Jakobsson, *Nano lett.*, 2003, **3**(5), 589–592.

46 C. N. Ramachandran and N. Sathyamurthy, *Chem. Phys. Lett.*, 2005, **410**(4–6), 348–351.

